

Statistical Analysis of a Posteriori Channel and Noise Distribution Based on HARQ Feedback

Wenhao Wu, *Student Member, IEEE*, Hans Mittelmann, Zhi Ding, *Fellow, IEEE*

Abstract

In response to a comment on one of our manuscript, this work studies the posterior channel and noise distributions conditioned on the NACKs and ACKs of all previous transmissions in HARQ system with statistical approaches. Our main result is that, unless the coherence interval (time or frequency) is large as in block-fading assumption, the posterior distribution of the channel and noise either remains almost identical to the prior distribution, or it mostly follows the same class of distribution as the prior one. In the latter case, the difference between the posterior and prior distribution can be modeled as some parameter mismatch, which has little impact on certain type of applications.

Index Terms

HARQ, posterior distributions, statistical analysis.

I. INTRODUCTION

In our recent manuscript [1], we studied the Modulation Diversity (MoDiv) design problem based on Hybrid Automatic Repeat reQuest (HARQ) Chase-Combining (CC) protocol. In this work, we approximate the bit error rate (BER) based on prior fading channel and noise distributions after each round of (re)transmission. One would argue that the need for the m -th (re)transmission implies that all previous transmissions have failed, thus the posterior channel and noise distribution would no longer be the same as the prior distribution. Consequently, it is natural to wonder when and how the posterior information, namely HARQ NACKs/ACKs, affects the channel and noise distribution.

There are a few works highlighting this difference between the prior and the posterior distributions [2][3][4], suggesting that adopting the prior distribution may lead to an overoptimistic estimation on the performance of HARQ. On the other hand, there are also abundant works about HARQ in fading channels that do not consider the posterior distribution, such as constellation

rearrangement [5], power allocation [6], rate selection [7] and so forth. As far as we know, it remains an open question under what conditions it is suitable or not to exploit the posterior distribution.

In this work, we study the posterior distribution of fading channels and noises in a practical LDPC-coded HARQ system under the general a priori assumptions of Rician fading channel and circularly symmetric complex Gaussian (CSCG) additive noises. By analyzing the posterior distribution with a series of three hypothesis tests on numerically generated channel and noise samples, we demonstrate that the posterior distribution may not significantly differ from the prior one, especially when each HARQ packet, or transport block (TB) in LTE terminology, experiences a few independent fading channel instances. Moreover, even when the coherence interval is large so that the instances of fading channels corresponding to each TB are more correlated, the posterior distribution may still follow the same type of distribution as the prior one except for some differences in parameters. This minor difference has negligible impact on specific applications such as modulation diversity (MoDiv) design [1][5]. To the best of our knowledge, the statistical approaches taken by this work to study the posterior fading channel and noise distribution in HARQ systems has not been reported in existing literature.

The rest of the paper is organized as follows: Section II discusses a few practical considerations why it may not be proper to adopt the posterior distribution in the studies of HARQ system. Section III describes our system model and how we generate the fading channel/noise samples corresponding to the posterior distribution for our hypothesis tests. In Section IV, we construct three hypothesis tests to analyze the posterior fading channel/noise distribution. The numerical results are provided in Section V. Finally, Section VI concludes this work.

II. BACKGROUNDS

One apparent reason why posterior distribution is not preferable is infeasibility, as a posterior analysis for HARQ system is usually too difficult unless one rely on some very restrictive, less practical settings and assumptions. For instance, [2] characterize the failure of transmissions with effective SNR and rate criteria, which on its own is a simplification and only numerical results are presented. Considering PAM constellations and maximum ratio combining (MRC), [3][4] attempts to explicitly formulate the error probability. However, the error probability based on Q function is an approximation, especially for practical high-order QAM modulations, and their analysis is based on instantaneous CSI and does not scale well for large number of

retransmissions. In practice, a transmission failure is declared by the cyclic redundancy check (CRC) when an error in the forward error correction (FEC) decoding result is detected. Such a complex event is difficult to characterize, let alone deriving a posterior channel distribution from it.

There is one questionable assumption common to all these works considering the posterior distribution in HARQ. The channel corresponding to a TB is always characterized by a single scalar effective SNR value, i.e. the entire TB experience a single instance of the fading channel and/or additive noise. As a practical example, in LTE system, each TB can be mapped to a maximum of 110 resource blocks (RB) of $0.5\text{ms} \times 180\text{kHz}$ [8, Table 7.1.7.2.1-1]. In the propagation condition [9, Table B.2-3], the coherence time could be as small as $\tau_c \approx 1/(4 \times 300\text{Hz}) = 0.833\text{ms}$ and the coherence bandwidth could be $B_c \approx 1/(2 \times 5000\text{ns}) = 100\text{kHz}$ [10, Table 2.1]. Consequently, each RB roughly experiences independent fading components and the univariate fading/noise instance per TB assumption is not satisfied. On the other hand, if each TB experiences N_{IF} independent fading channel instances, then the posterior channel/noise distribution should be defined over $\mathcal{O}(m \times N_{IF})$ complex variables, which easily becomes intractable.

The generalization from the abovementioned restrictive settings and assumptions which facilitates a posterior analysis for HARQ leads to the second—more essential but less obvious—reason why posterior distribution is not always worthy of exploiting: questionable necessity. In the rest part of this work, we will demonstrate that, in a more general and practical HARQ system, the posterior channel and noise distributions may not differ significantly from the prior ones, or the difference is too little to have visible impact on certain applications.

III. SYSTEM MODEL AND DATA GENERATION

A. Notations

We adopt the following notations throughout this work. $\Re\{\cdot\}$ and $\Im\{\cdot\}$ represent the real and imaginary part of a complex matrix. $[\mathbf{A}; \mathbf{B}]$ and $[\mathbf{A}, \mathbf{B}]$ represent vertical and horizontal concatenation of matrix \mathbf{A} and \mathbf{B} , respectively. Multivariate Gaussian distribution, multivariate CSCG distribution and chi-squared distribution with d degree-of-freedom are denoted with $\mathcal{N}(\cdot)$, $\mathcal{CN}(\cdot)$ and χ_d^2 . $\mathbf{0}_l$, $\mathbf{1}_l$ and \mathbf{I}_l denote the l -dimensional all-0 vectors, l -dimensional all-1 vectors and l -by- l -dimensional identity matrix. $|\cdot|$ and $\|\cdot\|_F$ represent the deterministic and Frobenius

norm of a matrix. $\text{diag}(\mathbf{a})$ represent the diagonal matrix whose diagonal elements are defined by vector \mathbf{a} .

B. System Model

We consider a simple Type-I HARQ system with Chase Combining (CC) under Rician fading channel and additive CSCG noise assumption. The received signal of the m -th retransmission ($m = 0$ represents the original transmission) is

$$y^{(m)} = h^{(m)} s^{(m)} + n^{(m)}, \quad (1)$$

where $s^{(m)}$ is the transmitted symbols originated from the same bit sequence across the (re)transmissions, and $n^{(m)} \sim \mathcal{CN}(0, \sigma^2)$ is the additive noise. The Rician channel can be modeled as [10, (2.55)]

$$h^{(m)} = \sqrt{\frac{K}{K+1}} \beta e^{j\theta} + \sqrt{\frac{1}{K+1}} \mathcal{CN}(0, \beta) \quad (2)$$

where K is the Rician factor, β is the mean power, and θ is the phase of the line-of-sight (LOS) component. We also assume that $n^{(m)}$ is independent across different samples and $h^{(m)}$ is independent across different (re)transmissions. Assuming all previous m decoding attempt have failed, after the m -th retransmission, the receiver makes another decoding attempt by combining the $m+1$ TBs received so far using a maximum likelihood (ML) detector, until $m > M$ where the HARQ transmission fails.

C. Data Generation

To analyze the posterior distribution of the fading channels and noises, we generate the channel/noise samples with a LDPC-coded system [11][12]. We assume that each TB contains 1 complete LDPC frame. Another tuning parameter, namely the number of independent fading channels per TB denoted as N_{IF} , is added to this system in order to test the impact of coherence interval on the posterior distribution. As shown in Fig. 1, for different m , we randomly generate a set of LDPC sessions, each consists of a encoding bit sequence and the fading channel/noise samples corresponding to the $(m+1)$ TBs. The LDPC-decoder then classify the LDPC sessions into two subsets based on whether the receiver sends a NACK (decoding failure) or ACK (decoding success) after the m -th retransmission, which represent the two classes of posterior distributions we are interested in.

Within each TB, the N_{IF} independent fading channel instances are periodically mapped to the L_s symbols. Among the L_s noise samples, we randomly sample N_{IF} in such a manner

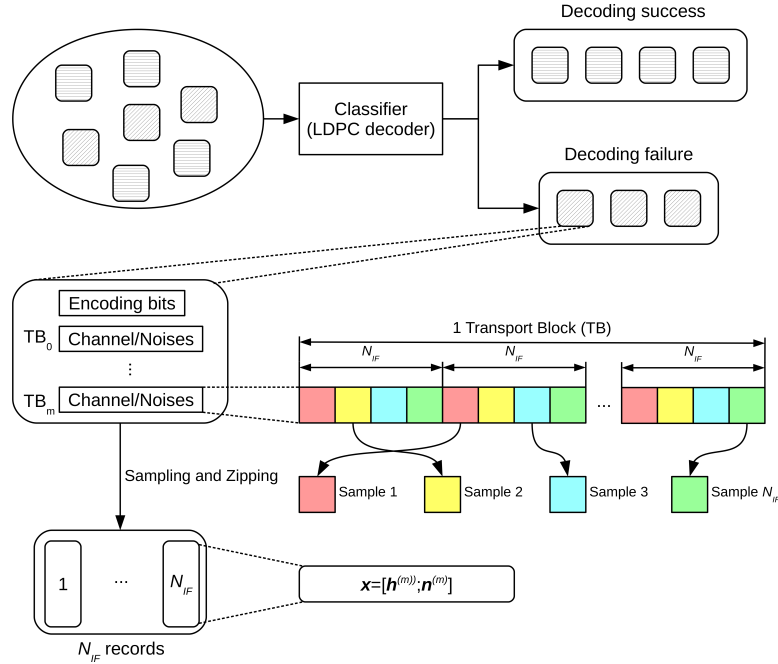


Fig. 1. The generation of datasets for the analysis on the posterior distribution of the fading channels and noises.

that the corresponding channel samples represent the N_{IF} independent fading channel instances completely. In this way we make sure that the number of channel samples and that of the noise samples are equally N_{IF} . Consequently, within each failed/successful HARQ session, a total number of $(m+1) \times N_{IF}$ groups of fading channels/noises are sampled. This groups of samples are then zipped across the $(m+1)$ (re)transmissions to construct N_{IF} records, each represented as a $2(m+1)$ -dimensional complex vector, or equivalently a $4(m+1)$ -dimensional real vector, in the form of

$$\mathbf{x} = [\Re\{\mathbf{h}^{(m)}\}; \Im\{\mathbf{h}^{(m)}\}; \Re\{\mathbf{n}^{(m)}\}; \Im\{\mathbf{n}^{(m)}\}] \quad (3)$$

where $\mathbf{h}^{(m)} = [h^{(0)}, \dots, h^{(m)}]$, $\mathbf{n}^{(m)} = [n^{(0)}, \dots, n^{(m)}]$.

In the next section, we carry out our hypothesis tests over a dataset of n records of \mathbf{x} , which is organized into a $4(m+1)$ -by- n matrix $\mathbf{X} = [\mathbf{x}_1, \dots, \mathbf{x}_n]$. For notational convenience we also decompose \mathbf{X} into four $(m+1)$ -by- n block matrices, i.e. $\mathbf{X} = [\mathbf{X}_{h,R}; \mathbf{X}_{h,I}; \mathbf{X}_{n,R}; \mathbf{X}_{n,I}]$, which represent the real and imaginary part of the channel and noise samples, respectively.

IV. DESIGN OF HYPOTHESIS TESTS

In this section, we construct a series of three binary hypothesis tests to see whether or on what conditions there is a significant difference between the posterior and the prior joint distribution of the fading channel and noise. The first test examines whether the posterior data and noise samples follow the same general type of distributions as the Rician channel and CSCG noise, i.e. whether \mathbf{x} follows Multi-Variate Normal (MVN) distribution. Once the MVN distribution is verified, the likelihood of \mathbf{X} can be evaluated, therefore a second test could further verify whether the distribution of \mathbf{x} is exactly the same as the prior distribution, i.e. whether the MVN parameters such as the mean and covariance matches those defined for the prior distribution. Should the second test fail, we fall back to a third test, which checks whether the distribution of \mathbf{x} still suggests an i.i.d Rician fading channel and CSCG noise model, though with potentially different parameters σ^2 , K , β and θ from the prior distribution. If so, the ML estimation of these four parameters could provide some insight into the difference between the posterior and prior distributions. These three hypothesis tests are detailed as follows.

A. Test 1: Multi-Variate Normality (MVN) Test

The first test is literally defined as:

$$\begin{aligned} \text{(Test 1)} \quad H_0 &: \mathbf{x} \text{ follows MVN distribution.} \\ H_1 &: \text{Otherwise.} \end{aligned} \tag{4}$$

Here we do not make any assumptions on the mean and covariance matrix of \mathbf{x} . As there are a wide variety of MVN tests with different characteristics [13] which may well reach contradictory conclusions over a same dataset, we adopt the the R package ‘MVN’ [14] which implements three popular MVN tests, namely Mardia’s test, Henze-Zirkler(HZ)’s test and Royston’s test.

B. Test 2: Parameter Matching Test

If Test 1 accept the null hypothesis H_0 , we can perform a second test to see whether \mathbf{x} has an identical distribution as the prior assumption. Specifically, assuming that \mathbf{x} is MVN distributed,

$$\begin{aligned} \text{(Test 2)} \quad H_0 &: \mathbf{x} \sim \mathcal{N}(\boldsymbol{\mu}_0, \boldsymbol{\Sigma}_0) \\ H_1 &: \text{Otherwise.} \end{aligned} \tag{5}$$

where

$$\boldsymbol{\mu}_0 = \left[\sqrt{\frac{K}{K+1}}\beta \cos \theta \mathbf{1}_{(m+1)}; \sqrt{\frac{K}{K+1}}\beta \sin \theta \mathbf{1}_{(m+1)}; \mathbf{0}_{2(m+1)} \right] \quad (6a)$$

$$\boldsymbol{\Sigma}_0 = \text{diag} \left(\left[\frac{\beta}{2(K+1)} \mathbf{1}_{2(m+1)}, \frac{\sigma^2}{2} \mathbf{1}_{2(m+1)} \right] \right) \quad (6b)$$

The following proposition reduces Test 2 into a chi-squared test:

Proposition 1. *Test 2 is equivalent to the following hypothesis test:*

$$\begin{aligned} (\text{Test 2(W)}) \quad H_0 : & -2 \ln(\Lambda_2) \sim \chi_{2(m+1)(4m+7)}^2 \\ H_1 : & \text{Otherwise.} \end{aligned} \quad (7)$$

as $n \rightarrow \infty$, where

$$\begin{aligned} -2 \ln(\Lambda_2) = & 2n(m+1) \ln \left(\frac{\beta \sigma^2}{4(K+1)} \right) + \frac{2(K+1)(\|\mathbf{X}_{h,R}\|_F^2 + \|\mathbf{X}_{h,I}\|_F^2)}{\beta} \\ & + \frac{2(\|\mathbf{X}_{n,R}\|_F^2 + \|\mathbf{X}_{n,I}\|_F^2)}{\sigma^2} - n \ln |\hat{\boldsymbol{\Sigma}}| - 4n(m+1) \end{aligned} \quad (8)$$

$$\hat{\boldsymbol{\Sigma}} = \frac{1}{n}(\mathbf{X} - \hat{\boldsymbol{\mu}}\mathbf{1}_n^T)(\mathbf{X} - \hat{\boldsymbol{\mu}}\mathbf{1}_n^T)^T, \quad \hat{\boldsymbol{\mu}} = \frac{1}{n}\mathbf{X}\mathbf{1}_n, \quad (9)$$

in which $\hat{\boldsymbol{\Sigma}}$, $\hat{\boldsymbol{\mu}}$ are the ML estimation of the covariance matrix and mean of \mathbf{x} from \mathbf{X} , respectively.

Proof. See Appendix. □

C. Test 3: Relaxed Parameter Matching Test

If Test 1 suggests that \mathbf{x} follows MVN distribution, but Test 2 suggests that it is not identical to the prior distribution, one would wonder whether the distribution of \mathbf{x} is still in a manageable form. A natural ‘‘guess’’ is that in this posterior distribution, the channels and noises across the $(m+1)$ (re)transmissions are still i.i.d Rician fading and CSCG distributed, respectively, except that the parameters σ^2 , K , β and θ are different from the prior distribution. In that case, we can examine the ML estimation of these parameters to see how different they are from the prior assumption, and whether certain applications are robust against this parameter mismatch between the posterior and prior distribution. This test is formulated as follows. Assuming that \mathbf{x} is MVN distributed,

$$\begin{aligned} (\text{Test 3}) \quad H_0 : & \mathbf{x} \sim \mathcal{N}(\tilde{\boldsymbol{\mu}}_0, \tilde{\boldsymbol{\Sigma}}_0) \\ H_1 : & \text{Otherwise.} \end{aligned} \quad (10)$$

where $\tilde{\boldsymbol{\mu}}_0$ and $\tilde{\boldsymbol{\Sigma}}_0$ are defined as in Eq. (6) with σ^2 , K , β , θ replaced by unknown parameters $\tilde{\sigma}^2$, \tilde{K} , $\tilde{\beta}$ and $\tilde{\theta}$, respectively.

Similar to Proposition 1, the following proposition reduces Test 3 to a chi-squared test:

Proposition 2. *Test 3 is equivalent to the following hypothesis test:*

$$\begin{aligned} \text{(Test 3(W)) } H_0 &: -2 \ln(\Lambda_3) \sim \chi_{2(m+1)(4m+7)-4}^2 \\ H_1 &: \text{Otherwise.} \end{aligned} \quad (11)$$

as $n \rightarrow \infty$, where

$$-2 \ln(\Lambda_3) = 2n(m+1) \ln \left(\frac{\hat{\beta} \hat{\sigma}^2}{4(\hat{K}+1)} \right) - n \ln |\hat{\boldsymbol{\Sigma}}| \quad (12)$$

in which

$$\hat{\sigma}^2 = \frac{\|\mathbf{X}_{n,R}\|_F^2 + \|\mathbf{X}_{n,I}\|_F^2}{n(m+1)}, \quad \hat{K} = \frac{\bar{h}_R^2 + \bar{h}_I^2}{\bar{\sigma}_h^2}, \quad \hat{\beta} = (\hat{K}+1)\bar{\sigma}_h^2, \quad \hat{\theta} = \arctan \frac{\bar{h}_I}{\bar{h}_R}, \quad (13)$$

are the ML estimation of $\tilde{\sigma}^2$, \tilde{K} , $\tilde{\beta}$ and $\tilde{\theta}$, respectively. The sample mean of the real and imaginary part and the sample variance of h are evaluated as

$$\bar{h}_R = \frac{\mathbf{1}_{m+1}^T \mathbf{X}_{h,R} \mathbf{1}_n}{n(m+1)}, \quad \bar{h}_I = \frac{\mathbf{1}_{m+1}^T \mathbf{X}_{h,I} \mathbf{1}_n}{n(m+1)}, \quad (14a)$$

$$\bar{\sigma}_h^2 = \frac{\|\mathbf{X}_{h,R} - \bar{h}_R \mathbf{1}_{m+1} \mathbf{1}_n^T\|_F^2 + \|\mathbf{X}_{h,I} - \bar{h}_I \mathbf{1}_{m+1} \mathbf{1}_n^T\|_F^2}{n(m+1)} \quad (14b)$$

Proof. See Appendix. □

V. NUMERICAL RESULTS

A. Simulation Settings

In our simulation, the Rician channel is specified with $\beta = 8$, $K = 1$ and $\theta = 0$. Each LDPC code word of length $L = 2400$ is mapped to 64-QAM constellation with the same Gray mapping for all (re)transmissions, therefore each TB consists of $L_s = 400$ symbols. The posterior fading channel and noise distribution is analyzed at $N_{IF} = 400, 100, 10, 1$ and $m = 0, 1, 2, 3$. For each pair of (N_{IF}, m) , we choose σ^2 such that around 50% of HARQ sessions fail and randomly generate $n \approx 10000$ records of \mathbf{x} for both the failed and successful sessions. The detailed parameters for each dataset are listed in Table I.

TABLE I
PARAMETERS FOR EACH NUMERICALLY GENERATED DATASET.

Dataset	N_{IF}	m	n_F	n_S	σ^2
1	400	0	10000	10000	0.13183
2	400	1	9600	10400	0.35892
3	400	2	9600	10400	0.58479
4	400	3	9600	10400	0.84421
5	100	0	10100	9900	0.13552
6	100	1	10300	9700	0.37154
7	100	2	10100	9900	0.59772
8	100	3	10200	9800	0.83946
9	10	0	10240	9760	0.13804
10	10	1	9980	10020	0.37154
11	10	2	9970	10030	0.60534
12	10	3	10200	9800	0.84140
13	1	0	10232	9768	0.18408
14	1	1	9834	10166	0.40738
15	1	2	9915	10085	0.64565
16	1	3	9628	10372	0.86099

B. Hypothesis Test Results

The p -values of Test 1 over all datasets are shown in Table II. For $N_{IF} = 1$, the posterior distribution indeed appears to be of different type from the prior distribution. However, for $N_{IF} = 10, 100, 400$, there is strong evidence indicating that the fading channels and noises still follow MVN distribution. This is especially true for larger N_{IF} (100, 400) where all the three MVN tests support the null hypothesis, and the failed sessions in which we are more interested since they are supposed to be used in the posterior analysis.

The p -values of Test 2 and Test 3 are shown in Table III. As we can see, for larger N_{IF} (100, 400), Test 2 suggests that the posterior distribution are likely to be the same as the prior distribution. For intermediate $N_{IF} = 10$, although Test 2 rejects the null hypothesis, in 3 of the 4 failed sessions Test 3 indicates that the posterior distribution can be still viewed as independent

TABLE II

TEST 1: MVN TESTS. THE p -VALUES CORRESPONDING TO REJECTED NULL HYPOTHESES ($p < 0.01$) ARE COLORED RED.

Dataset	Failed sessions				Successful sessions			
	Mardia-skew	Mardia-kurt	HZ	Royston	Mardia-skew	Mardia-kurt	HZ	Royston
1	0.03707	0.5945	0.1044	0.09758	0.3086	0.3285	0.1810	0.5405
2	0.2869	0.6188	0.9854	0.2496	0.7373	0.7304	0.8650	0.2439
3	0.7019	0.05709	0.9187	0.4361	0.7523	0.1693	0.7661	0.1821
4	0.7590	0.7925	0.5395	0.2098	0.6935	0.4394	0.9345	0.8580
5	0.2720	0.1313	0.2117	0.9635	0.6373	0.7678	0.1052	0.1444
6	0.8645	0.2425	0.4166	0.7259	0.5645	0.7191	0.1495	0.9247
7	0.6248	0.9021	0.9473	0.4020	0.1583	0.7446	0.4879	0.8501
8	0.1308	0.7417	0.8127	0.1612	0.9160	0.5376	0.3666	0.3905
9	6.172e-10	0.02679	8.639e-13	0.01571	7.459e-20	0.04260	6.661e-16	2.562e-4
10	9.934e-4	0.3654	0.01845	0.02896	7.720e-8	0.8683	2.494e-4	0.01850
11	0.3692	0.03412	0.4131	0.7423	0.1039	0.1747	0.5589	0.8595
12	0.6141	0.9034	0.7274	0.04015	0.8693	0.1940	0.6021	0.4035
13	1.414e-229	9.191e-6	0	2.753e-27	0	0	0	1.646e-22
14	5.118e-236	4.239e-8	0	2.613e-22	5.620e-269	1.800e-7	0	3.049e-12
15	5.052e-156	6.174e-10	0	2.596e-14	3.303e-243	0.01597	0	3.497e-10
16	3.235e-131	3.478e-10	0	2.356e-13	2.006e-173	0.9775	0	1.130e-6

Rician fading channels and CSCG noises. A closer look at the ML estimation results in Table IV reveals that the posterior $\hat{\beta}$ and $\hat{\theta}$ are almost the same as the prior ones. However, the posterior Rician channel has smaller $\hat{\beta}$ and \hat{K} for the failed sessions, and larger ones for the successful sessions, as compared to the prior parameters. In general, this gap increases as N_{IF} and m decreases. Finally, when $N_{IF} = 1$, despite the rejection of MVN hypothesis so that Test 2 and Test 3 are meaningless, the ML estimation in Eq. (13) still serves as the empirical mean square of the fading channel and the noises. The noise power is still almost the same as the prior distribution, while the channel power is much smaller and much larger for the failed and successful sessions, respectively, than the prior one.

TABLE III

TEST 2 AND TEST 3, PARAMETER MATCHING TESTS (EXACT AND RELAXED). THE p -VALUES CORRESPONDING TO REJECTED NULL HYPOTHESES ($p < 0.01$) ARE COLORED RED.

Dataset	Failed sessions		Successful sessions	
	Test 2	Test 3	Test 2	Test 3
1	0.1350	0.2781	0.04330	0.3123
2	0.1614	0.5014	0.9206	0.9258
3	0.1125	0.1436	0.1333	0.2081
4	0.4806	0.4941	0.9758	0.9734
5	0.01253	0.04575	1.358e-11	7.713e-3
6	0.06204	0.3005	0.02778	0.6205
7	0.2207	0.6941	0.3504	0.7882
8	0.4434	0.9241	0.01312	0.2772
9	0	5.236e-4	0	6.890e-10
10	0	0.02033	0	1.264e-5
11	0	0.3848	0	6.695e-8
12	0	0.3573	0	6.697e-3
13	0	0	0	0
14	0	0	0	0
15	0	0	0	0
16	0	0	0	0

C. The Impact of Parameter Mismatch on MoDiv Design

For the intermediate $N_{IF} = 10$, the hypothesis tests results suggest that the difference between the posterior and prior distribution can be viewed mostly as a parameter mismatch and the main difference is on the channel power β and Rician factor K . As an example of how this parameter will affect certain type of application, we consider the Modulation Diversity (MoDiv) design problem in [1][5]. we compare the MoDiv design based on prior distribution ($\beta = 8$ and $K = 1$) and that based on an artificial posterior distribution for the failed sessions ($\beta = 6.5$ and $K = 0.8$), and compare their actual BER performance over the artificial posterior distribution. The simulation results are shown in Fig. 2. Despite that the gap in K and β between

TABLE IV
THE ML ESTIMATION OF THE PARAMETERS OF RICIAN CHANNEL AND CSCG NOISE FROM TEST 3.

Dataset	Failed sessions				Successful sessions			
	$\hat{\beta}$	\hat{K}	$\hat{\theta}$	$\hat{\sigma}^2$	$\hat{\beta}$	\hat{K}	$\hat{\theta}$	$\hat{\sigma}^2$
1	7.830	0.9883	6.391e-3	0.1330	8.137	1.015	-9.221e-3	0.1284
2	7.902	0.9899	-6.634e-3	0.3664	8.063	1.017	-2.772e-3	0.3572
3	7.936	0.9920	4.855e-3	0.5904	8.027	1.010	-8.987e-3	0.5797
4	8.017	0.9954	-6.380e-3	0.8479	8.011	1.013	-1.333e-3	0.8468
5	7.831	0.9793	1.878e-3	0.1381	8.505	1.078	-3.657e-3	0.1336
6	7.827	0.9952	-4.889e-3	0.3733	8.232	1.017	-0.01006	0.3683
7	7.854	0.9692	-3.902e-3	0.6032	8.158	1.022	-7.301e-3	0.5987
8	7.822	0.9765	-3.594e-3	0.8413	8.194	1.035	2.162e-4	0.8369
9	6.760	0.8111	-3.474e-3	0.1418	9.262	1.261	4.441e-3	0.1373
10	6.965	0.8721	-3.151e-3	0.3726	9.046	1.142	6.379e-3	0.3740
11	7.105	0.8999	-2.120e-3	0.6079	8.936	1.118	1.622e-3	0.6039
12	7.240	0.9198	4.991e-4	0.8442	8.758	1.078	6.637e-3	0.8363
13	2.958	0.6028	0.01418	0.1860	13.20	2.101	-5.829e-3	0.1876
14	4.206	0.7147	-5.320e-3	0.4027	11.67	1.522	-2.713e-3	0.4038
15	4.911	0.7668	-3.975e-4	0.6421	11.06	1.381	2.002e-3	0.6428
16	5.247	0.7996	1.944e-3	0.8598	10.56	1.305	-2.141e-3	0.8551

the two distributions is larger than suggested by Table III, there is hardly any difference in BER performance, suggesting that MoDiv design is an application somehow robust against the difference between the posterior and prior distribution.

D. Remarks

These numerical results demonstrate that, except when N_{IF} is very small, the posterior distribution conditioned on the failure of all previous HARQ transmissions is not so different from the prior distribution, or this difference is too trivial to affect certain type of applications. In many existing works on HARQ, no assumption on N_{IF} or the coherence interval is made except that the channels are independent across retransmissions, and no FEC/CRC scheme or

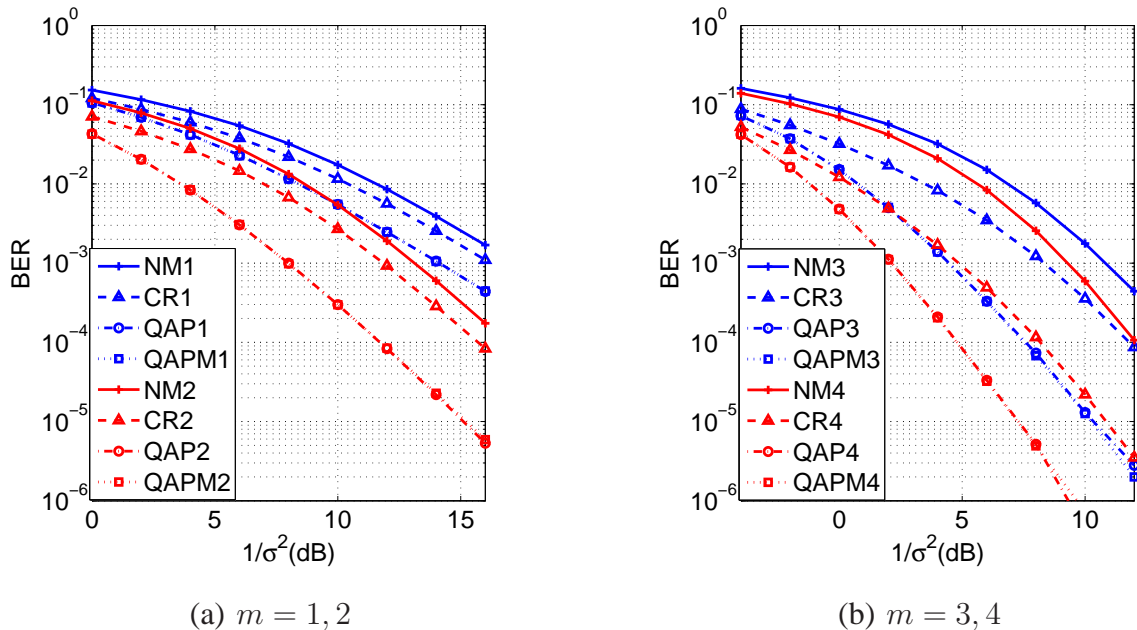


Fig. 2. The Monte-Carlo simulated uncoded BER for different m . NM_m and CR_m are two benchmark modulation diversity schemes. $QAPM_m$ represents the QAP-based MoDiv scheme designed using prior distribution but tested on the posterior distribution, while QAP_m represents the QAP-based MoDiv scheme designed and tested on the posterior distribution.

transport block structure is specified. Attempt to use the posterior distribution is likely to be unfounded. On the other hand, when we introduce more general, practical assumptions to the HARQ systems being studied, it is usually difficult, if not impossible, to derive the posterior distribution.

VI. CONCLUSION

This work investigates the posterior fading channel and noise distribution in a HARQ system conditioned on the HARQ feedbacks. We design three hypothesis tests, demonstrating with channel and noise samples generated from a practical LDPC-coded HARQ system that, unless the coherence interval is large or the number of independent fading instances per TB is small, the posterior distribution is not so different from the prior distribution, or the difference is so small that it has negligible effect on certain types of applications. To some extent, this work justifies the seemingly lax use of prior distribution in many existing works about HARQ.

APPENDIX

PROOF FOR PROPOSITION 1 AND PROPOSITION 2

The proof is simply an adoption of Wilks' theorem [15]. The log-likelihood of observing \mathbf{X} under MVN distribution $\mathcal{N}(\boldsymbol{\mu}, \boldsymbol{\Sigma})$ is

$$\ln(L(\boldsymbol{\mu}, \boldsymbol{\Sigma}|\mathbf{X})) = -\frac{n}{2} \ln |\boldsymbol{\Sigma}| - \frac{1}{2} \text{tr}(\boldsymbol{\Sigma}^{-1}(\mathbf{X} - \boldsymbol{\mu}\mathbf{1}_n^H)(\mathbf{X} - \boldsymbol{\mu}\mathbf{1}_n^H)^H) + C \quad (15)$$

where C is a constant. The parameter space $\Theta = \{(\boldsymbol{\mu}, \boldsymbol{\Sigma})\}$ has a dimension of $2(m+1)(4m+7)$. Its supremum

$$\begin{aligned} \sup\{\ln(L(\boldsymbol{\mu}, \boldsymbol{\Sigma}|\mathbf{X}))\} &= \ln(L(\hat{\boldsymbol{\mu}}, \hat{\boldsymbol{\Sigma}}|\mathbf{X})) \\ &= -\frac{n}{2} \ln |\hat{\boldsymbol{\Sigma}}| - 2n(m+1) + C \end{aligned} \quad (16)$$

where $\hat{\boldsymbol{\mu}}, \hat{\boldsymbol{\Sigma}}$ are defined in Eq. (9).

Under the null hypothesis of Test 2, the parameter space $\Theta_0^{(T2)}$ has 0 dimensionality, the supremum of log-likelihood is

$$\begin{aligned} &\sup\{\ln(L(\boldsymbol{\mu}, \boldsymbol{\Sigma}|\mathbf{X})) : (\boldsymbol{\mu}, \boldsymbol{\Sigma}) \in \Theta_0^{(T2)}\} \\ &= \ln(L(\boldsymbol{\mu}_0, \boldsymbol{\Sigma}_0|\mathbf{X})) \\ &= -n(m+1) \ln \left(\frac{\beta\sigma^2}{4(K+1)} \right) - \frac{(K+1)(\|\mathbf{X}_{h,R}\|_F^2 + \|\mathbf{X}_{h,I}\|_F^2)}{\beta} - \frac{\|\mathbf{X}_{n,R}\|_F^2 + \|\mathbf{X}_{n,I}\|_F^2}{\sigma^2} + C \end{aligned} \quad (17)$$

therefore according to Wilks' theorem, as $n \rightarrow \infty$

$$\begin{aligned} -2 \ln(\Lambda_2) &= 2 \left(\sup\{\ln(L(\boldsymbol{\mu}, \boldsymbol{\Sigma}|\mathbf{X}))\} - \sup\{\ln(L(\boldsymbol{\mu}, \boldsymbol{\Sigma}|\mathbf{X})) : (\boldsymbol{\mu}, \boldsymbol{\Sigma}) \in \Theta_0^{(T2)}\} \right) \\ &\sim \chi_{2(m+1)(4m+7)}^2 \end{aligned} \quad (18)$$

Under the null hypothesis of Test 3, the parameter space $\Theta_0^{(T3)}$ has a dimensionality of 4, the supremum of log-likelihood is

$$\begin{aligned} &\sup\{\ln(L(\boldsymbol{\mu}, \boldsymbol{\Sigma}|\mathbf{X})) : (\boldsymbol{\mu}, \boldsymbol{\Sigma}) \in \Theta_0^{(T3)}\} \\ &= \ln(L(\hat{\boldsymbol{\mu}}_0, \hat{\boldsymbol{\Sigma}}_0|\mathbf{X})) \\ &= -n(m+1) \ln \left(\frac{\hat{\beta}\hat{\sigma}^2}{4(\hat{K}+1)} \right) - 2n(m+1) + C \end{aligned} \quad (19)$$

where $\hat{\boldsymbol{\mu}}_0, \hat{\boldsymbol{\Sigma}}_0$ are defined as in Eq. (6) with $\sigma^2, K, \beta, \theta$ replaced by the ML estimation $\hat{\sigma}^2, \hat{K}, \hat{\beta}, \hat{\theta}$, respectively. Similar to the case of Test 2, as $n \rightarrow \infty$

$$\begin{aligned} -2 \ln(\Lambda_3) &= 2 \left(\sup\{\ln(L(\boldsymbol{\mu}, \boldsymbol{\Sigma}|\mathbf{X}))\} - \sup\{\ln(L(\boldsymbol{\mu}, \boldsymbol{\Sigma}|\mathbf{X})) : (\boldsymbol{\mu}, \boldsymbol{\Sigma}) \in \Theta_0^{(T^3)}\} \right) \\ &\sim \chi_{2(m+1)(4m+7)-4}^2 \end{aligned} \quad (20)$$

REFERENCES

- [1] W. Wu, H. Mittelmann, and Z. Ding, "Modulation design for two-way amplify-and-forward relay HARQ," submitted for publication.
- [2] J. Gu, Y. Zhang, and D. Yang, "Modeling conditional FER for hybrid ARQ," *IEEE Commun. Lett.*, vol. 10, no. 5, pp. 384–386, May 2006.
- [3] H. Long, W. Xiang, S. Shen, Y. Zhang, K. Zheng, and W. Wang, "Analysis of conditional error rate and combining schemes in HARQ," *IEEE Trans. Signal Process.*, vol. 60, no. 5, pp. 2677–2682, May 2012.
- [4] R. Alkurd, R. Shubair, and I. Abualhaol, "Modeling conditional error probability for hybrid decode-amplify-forward cooperative system," in *Proc. IEEE Wireless Commun. Netw. Conf. (WCNC)*, March 2015, pp. 7–12.
- [5] H. Samra, Z. Ding, and P. Hahn, "Symbol mapping diversity design for multiple packet transmissions," *IEEE Trans. Commun.*, vol. 53, no. 5, pp. 810–817, May 2005.
- [6] T. Chaitanya and E. Larsson, "Adaptive power allocation for HARQ with Chase combining in correlated rayleigh fading channels," *IEEE Wireless Commun. Lett.*, vol. 3, no. 2, pp. 169–172, April 2014.
- [7] H. Jin, C. Cho, N.-O. Song, and D. K. Sung, "Optimal rate selection for persistent scheduling with harq in time-correlated nakagami-m fading channels," *IEEE Trans. Wireless Commun.*, vol. 10, no. 2, pp. 637–647, February 2011.
- [8] 3GPP TS36.213, "Evolved Universal Terrestrial Radio Access (E-UTRA): Physical layer procedures," Sep. 2015, v12.7.0.
- [9] 3GPP TS36.141, "Evolved Universal Terrestrial Radio Access (E-UTRA): Base Station (BS) conformance testing," Oct. 2015, v13.1.0.
- [10] D. Tse and P. Viswanath, *Fundamentals of wireless communication*. Cambridge university press, 2005.
- [11] B. Hochwald and S. ten Brink, "Achieving near-capacity on a multiple-antenna channel," *IEEE Trans. Commun.*, vol. 51, no. 3, pp. 389–399, March 2003.
- [12] M. Valenti. (2007) The coded modulation library. [Online]. Available: <http://www.iterativesolutions.com>
- [13] C. J. Mecklin and D. J. Mundfrom, "A Monte Carlo comparison of the Type I and Type II error rates of tests of multivariate normality," *Journal of Statistical Computation and Simulation*, vol. 75, no. 2, pp. 93–107, 2005.
- [14] S. Korkmaz, D. Goksuluk, and G. Zararsiz, "Mvn: An r package for assessing multivariate normality," *A peer-reviewed, open-access publication of the R Foundation for Statistical Computing*, p. 151, 2014.
- [15] S. S. Wilks, "The large-sample distribution of the likelihood ratio for testing composite hypotheses," *The Annals of Mathematical Statistics*, vol. 9, no. 1, pp. 60–62, 1938.